Chemical Science

Accepted Manuscript

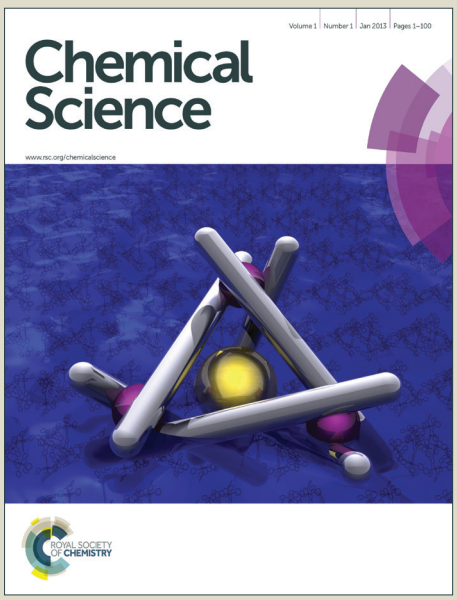

ROYAL SOCIETY OF CHEMISTRY

www.rsc.org/chemicalscience

ARTICLE TYPE www. rsc.org/xxxxxx | XXXXXXXX

Resolving Molecular Orbitals Self-decoupled from Semiconductor Surfaces

Jing Hui He,[ab] Wei Mao,[ab] Wei Chen,[acb] Kai Wu,[db] Han Song Cheng,[a] and Guo Qin Xu[ab]*

Received Xth XXXXXXXXXX 20XX, Accepted Xth XXXXXXXXX 20XX
First published on the web Xth XXXXXXXXXX 200X
DOI: 10.1039/b000000x

Resolving orbitals using scanning tunneling microscopy (STM) provides an in-depth understanding of the chemical and electronic nature of molecule/substrate junctions. Most orbital resolving work was performed for molecules physisorbed on metal surfaces by inserting interfacial layers to decouple the interaction between the molecules and substrates. It remains challenging to image the orbitals of molecules directly chemisorbed on native surfaces because the linking chemical bonds likely induce severe coupling. Here we demonstrate that the π orbitals of the phenyl rings from chemisorbed nitrosobenzene on Ge(100) are electronically decoupled from the semiconductor surface and can be resolved by STM. Four types of dumbbell-like molecular features are imaged, corresponding to the intradimer and interdimer [2+2] nitrosoadducts. In these products, nitrosobenzene binds to Ge(100) through its N=O group, which spatially separates and electronically decouples the phenyl ring (C_6H_5-) from the substrate. Theoretical calculations and STM simulation reveal that the dumbbell-like features resemble the occupied π orbitals of benzene. Our results show that electronic decoupling and orbital resolving can be achieved for molecules binding to highly reactive surfaces via sacrificing a double bond as the anchoring/spacing group.

Introduction

Adsorption of molecules on surfaces has received extensive attention for potential applications in molecule-based devices.[1] Understanding and tuning the chemical and electronic nature of organic/substrate junctions are essential steps towards their implementation in real devices.[2] In this context, scanning tunneling microscopy (STM) has been proved to be a powerful tool because of its capability of spatially resolving individual organic adsorbates in an Å scale. In addition, it has been demonstrated that the orbital information of the adsorbed molecules can be extracted by STM.[3,4] Although orbitals are not observables in quantum theories, experimentally, their electron density distributions and energy levels are observable using STM.[5–7] Once the molecular orbitals are "imaged", the reaction mechanisms[8,9]as well as the electronic properties of an adsorbate can be learned.[3,10] This knowledge at the molecule/substrate junctions(s) is essential in design/optimazation/implementation of molecular devices.[11,12] However, spatially resolving orbitals by STM remains technically challenging.[13] Apart from the need of a good STM tip as well as low operational temperatures,[3,6,14–17] it is critical to select and design the substrates and molecules so that their electronic states are decoupled from each other. Thus most successful orbital resolving studies are limited in physisorbed molecules on substrates, where delicate insertion of ultrathin insulating NaCl films,[3,10] self-assembled phthalocyanine monolayers,[16,18,19] semi-metallic graphene sheets[20] and hydrogen passivation layers[21] were used to prevent the electronic coupling. Meanwhile, the molecules chosen in these works are flat-lying polycyclic aromatics and their derivatives, such as perylene,[22] pentacene[3,10] and metal-Phthalocyanines.[16,18,19] The large dimension and high density of states of the delocalized π orbitals of these molecules favor the spatial mapping by STM. None of small aromatics such as single aromatic rings has been imaged with orbital resolution. Despite their inspiring success, these methods still suffer from low operational temperatures, complex surface preparation procedures or low efficiency for electron transportation,[12] therefore unviable for future practical device applications.

In contrast to dominating reports on physisorption systems, orbital imaging has rarely been reported for molecules directly chemisorbed on native surfaces. Compared to physisorbed adsorbates, chemisorbed molecules are anchored to the substrates through chemical bonds (mainly covalent) with sufficient thermal and mechanical stabilities, as well as shorter electron channel.[12] However, the electronic coupling between the substrates and adsorbates also becomes severe and often inevitable. The chemisorbed molecules are perturbed or even deformed by the resulting chemical bonds,[23] unable to sustain and present their molecular orbitals.[24] In order to resolve molecular orbitals in chemisorption system, one has to solve the paradox between the electronic decoupling and chemical bonding. In addition, the solution also represents the effort to retain and exploit the designed molecular properties/functional groups from reactive surfaces.

In this work, we resolved the molecular orbitals of nitrosobenzene chemisorbed on a clean semiconductor surface, which has highly reactive dangling bonds and usually binds molecules through covalent bonds.[25,28] Nitrosobenzene (C_6H_5-N=O) binds to the Ge(100) surface through its N=O group, leaving the phenyl ring spatially and electronically self-decoupled from the substrate. Therefore the occupied π orbitals of the phenyl ring are retained and resolved by STM at room temperature.

Experimental and computational details

The STM experiments were performed on an Omicron variable-temperature STM mounted in an observation chamber attached to a main ultra-high vacuum chamber with a base pressure of 1×10^{-8} Pa. The Ge(100) sample was cut from an n-doped, single side polished wafer with a resistivity of 1-2 Ω·cm and a size of 12 mm×2 mm×0.5 mm. The clean Ge surface was obtained by several cycles of 1000 V Ar^+ sputtering and flashing to 1000 K. Nitrosobenzene (99%, Sigma-Aldrich Chemical) was purified via six freeze-pump-thaw cycles before being dosed onto the Ge(100) sample. The STM tips were made from electrochemically etched tungsten wires, the dosing pressure is 1×10^{-8} Pa for two minutes. The dosing aperture is about 0.5 m away from the STM tip. In STM experiments, the dosing is in-situ during STM scanning, and the coverage was directly monitored by STM.

The DFT calculations were performed using the Vienna ab initio simulation package(VASP).[29,30] A c(4×2) slab model of six layers of Ge was used to simulate the Ge(100) surface. This slab includes four dimers on the surface, three layers in the middle and two frozen layers at the bottom. The generalized gradient approximation (GGA) with Perdew-Burke-Ernzerhof (PBE) parameterizations was used to estimate the exchange-correlation effect.[31] The projector augmented wave (PAW) pseudopotentials method with a kinetic energy cut off 300 eV was employed. Brillouin Zone sampling was performed on a 2×4×1 Γ-centered Monkhorst-Pack grid. A gaussian smearing 0.01 eV was used to accelerate the SCF convergence. The force criterion for convergence during the geometric optimizations is 0.01 eV/Å. The rotation barriers of phenyl rings through C-N bonds are via calculating the single point energies of a series of structures with variable O-N-C-C torsion torsion angles. The barriers, if calculated based on the constrained relaxation method, should be lower than the above values.

The STM images were simulated by applying the Tersoff-Hamann approximation.[7] To render the molecule/substrate system orbitals, the isosurfaces of partial density of states in a narrow energy window (±0.05 eV) at the selected peak positions were presented. To plot the molecular orbitals, DMol^3 [32,33] in Materials Studio (version 5.5) of Accelrys was employed. Spin unrestricted DFT calculations with GGA-PBE approximation was applied. Other parameters were set as close to the slab model as possible.

Results and discussion

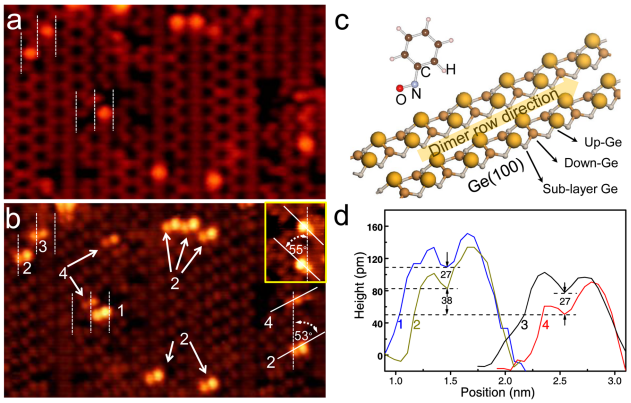

Fig. 1 STM images of a Ge(100) surface during adsorption of nitrosobenzene molecules at a normal resolution (a) and submolecular resolution (b). The numbers **1**, **2**, **3** and **4** mark four types of dumbbell-like features. The vertical dash lines refer to the dimer troughs. An alternative orientation of the dumbbells of 2 and 4 is shown in the inset. (c) Structural models of nitrosobenzene molecule and the Ge(100) surface. The deeper Ge atoms of Ge(100) are not shown for clarity. (d) Line profiles of the marked features in (b) along their axes of symmetry. Scanning area: 70×80 Å. *I*= 200 pA, *V*= -1.6 V.

STM imaging was carried out while dosing molecules onto a clean Ge(100) sample in an ultra-high vacuum chamber at room temperature. Figure 1a shows a STM image of Ge(100) after dosing nitrosobenzene, where the zig-zag chains and straight stripes refer to Ge buckled dimers.[34] There are unevenly distributed dangling bonds on Ge dimer atoms, which probably result in multiple products when reacting with molecules. Like most of the STM images obtained on semiconductor surfaces, Figure 1a exhibits adsorbed molecules as bright elliptic spots. At this "normal" resolution, these adsorption products can only be roughly distinguished from the binding sites, but their detailed binding mechanisms remain mysterious due to the limited intramolecular details.

Rather than conducting STM scanning after dosing, we simultaneously scanned the surface when dosing molecules. Figure 1b shows a typical image of the same area as in Figure 1a at a submolecular resolution, because all molecular elliptical spots split into "dumbbells". The nodal planes of these dumbbells have a uniform angle of about 53° relative to the dimer row direction (vertical lines in Figure 1). This uniform orientation was found to be independent of substrate terraces,

even though the alternative terraces of Ge(100) are of perpendicular dimer row directions. However, the dumbbells could rotate themselves by 108° anticlockwisely and convert to their "enantiomers" in another scanning round. The variable orientation indicates that the molecular fragment being imaged by STM likely connects to the substrate through a rotatable bond. The orientational alignment may result from external electric fields, which we will briefly discuss later.

Before we discuss the structural details of these dumbbell-like features, it is worthy to check how the resolution in Figure 1b was improved. In contrast to the dumbbell-like molecular features, the background Ge dimer atoms, particularly those at the edge of the dim defects in Figure 1b, only sharpened but not split. This clearly excludes the possible double tip effect induced by two tunneling points on the tip apex, which would duplicate or smear not only the protrusions but also the background atoms, particularly for those edge atoms near the defects within the terraces.[35,36] Thus these "dumbbells" should reflect intramolecular structures of the adsorbates. Given the same sample and scanning conditions in Figures 1a and 1b (the same scanning area, scanning direction, tunneling bias and current), the improvement of resolution can only be attributed to the change of the STM tip state. We carefully searched the scanning area for the points where the resolution was transiting from the normal to the submolecular (or vice versa, Figure S1) by analyzing the STM images pixel by pixel (Figure S2 and its related description), and we compared these points in consecutive STM images right before and after this submolecular state. Neither exotic atom/particle was found to drop from the tip to substrate near these transiting points, nor was surface atom picked up by the tip because no atomic defect generated at those points. Thus, we propose that the submolecular resolution should only be induced via modification of the tip apex by external molecules coming from the vacuum.

Improvement of STM resolution by capping STM tips with molecules was widely reported,[3,6,14] despite the difficulty in resolving the exact tip-molecule attaching mechanisms. Generally, it is believed that those attached molecules offer single s-type orbital for new tunneling channel,[37] by which the STM images approximately resemble the modulus squared of the sample orbital(s) near the Fermi level.[6,7] However, the inset of Figure 1b shows another asymmetric dumbbell-like appearance with an alternative orientation. This indicates that the STM tip apex in submolecular-resolution state is likely composed of an asymmetric and metastable collection of s-type orbitals,[38] which differs the molecular features from that of single s-orbital tip while retaining the nodal planes. The most plausible explanation in our experiments is that nitrosobenzene binds to the tip tungsten atoms through N and O atoms as they have high affinity to transition metals. Via in situ dosing, the submolecular resolutions could be achieved repeatedly. The biased tips during scanning may readily attract molecules while in situ dosing.[39]

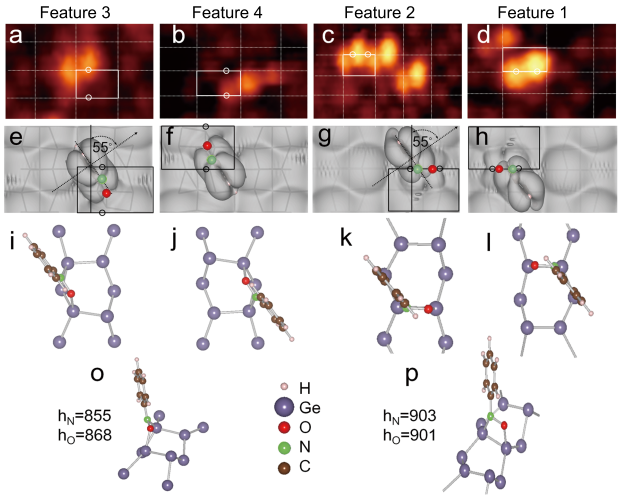

Fig. 2 (a)-(d) Experimental STM images adapted from Figure 1b. (e)-(h) Simulated STM images at -1.6 V of structures (i)-(l), respectively. (i) and (j) Interdimer nitrosoadduct model and its side view (o). (k) and (l) Intradimer nitrosoadduct model and its side view (p). The solid rectangles in (a)-(h) are 2×1 reconstructed unit cells of Ge(100), where the empty circles mark the reacted dimer atoms. The positions of N and O atoms are also highlighted by balls. h_N and h_O in (o) and (p) are the heights of N and O atoms in the unit of pm, relative to the bottom Ge layer.

Under the submolecular resolution, the adsorption features can now be more precisely located and classified compared to the normal resolution as in Figure 1a. Four types of features **1**, **2**, **3** and **4** are identified according to their heights (Figure 1d) and locations (Figures 2a-2d, referring to the centers of the dumbbells). Among these features, **1** is the highest, and its center coincides with the center of a dimer. The major type **2** is lower than **1** by 27 pm, with its center on the left side of a dimer. In contrast to the above types, **3** and **4** locate themselves in the middle of dimer troughs. **4** is the lowest, lower than **3** by 27 pm, and **2** by 38 pm. Types **1**, **2** and **4** all have their left parts of the dumbbells lower than the right halves by about 30 pm, while **3** is of its left part higher. In short, the dumbbell-like appearance at the submolecular resolution offers us more structural details, which can help us to more reliably interpret the binding mechanisms and electronic structures of the adsorbed molecules.

As for molecular devices, it is important to understand and tune the geometric and electronic structures of a molecule after being attached to substrates. Density functional theory (DFT) calculation complements experimental STM study with its ability to search for possible adsorption structures and to simulate their STM images. Based on DFT calculation, the four types of dumbbell-like features can be assigned to two ad-

sorption products. Features **3** and **4** are both in dimer troughs (Figures 2a and 2b). They are assigned to an interdimer [2+2] nitrosoadduct shown in Figure 2o. Figures 2i and 2j show the top views of this interdimer adduct with their orientations differing by 180°. In this configuration, the nitroso group (-N=O) reacts with the paired end-bridge of two adjacent surface dimers within the same dimer row, leaving the phenyl ring intact above the dimer trough. Simulated STM images at the bias of -1.6 V (Figures 2e and 2f) clearly show the existence of nodal planes. The nodal plane of each simulated "dumbbell" coincides with the phenyl ring plane, thus two halves of the dumbbell are tentatively attributable to the side view of the phenyl ring's π orbital(s). The sizes of orbitals lobes separated by the nodal planes in calculation are generally smaller than that observed in the experiments[40] because the tip shape is not considered in the Tersoff-Hamman approximations. Similarly, Features **2** and **1** are related to intradimer [2+2] nitrosoadducts in Figure 2p with opposite orientations (Figures 2k and Figure 2i). In intradimer state, each nitroso group adds to a single dimer, whereas the phenyl ring remains intact, standing on top of dimer atoms. Both intradimer and interdimer adducts have a similar orientation (55°) relative to the dimer row, in tight agreement with Figures 2a and 2b, respectively. It is also worthy to compare the heights of two nitrosoadducts by checking the position of N, which is anchored by the Ge substrate and supports the intact phenyl ring in all structures. Our structural models indicate that the intradimer product is higher than the interdimer adduct (903-855=38 pm, in Figure 2o and 2p). This is in line with the experimental line profiles in Figure 1d, further supporting our proposed adsorption mechanisms. This excellent match demonstrates that the dumbbell-like features possess more structural information that is inaccessible at the normal STM resolution, and the interpretation based on these features should be more reliable.

The above [2+2]-cycloaddition mechanism is supported by previous studies as well as our calculations. Nitrosobenzene is composed of a phenyl ring and a nitroso group. Both may react with Ge(100), which is of highly reactive double-bonding dimers. However, the formation of two nitrosoadducts is supported by a similar addition reaction when nitrosobenzene adsorbs on Si(100).[44] In addition, benzene is not reactive on Ge(100) at room temperature.[45] Thus it is unlikely that nitrobenzene reacts with Ge(100) via the phenyl ring. As a typical [2+2] cycloaddition on group IV surfaces,[46] the nitroso group (-N=O) reacting with Ge dimer should be barrierless (also confirmed by our calculation) and facile to occur at room temperature. Our calculations show that adsorption energies of interdimer and intradimer nitrosoadducts are 1.35 and 1.65 eV, respectively. The discrepancy in adsorption energy is attributable to the loss of dimer bulking energy.[47] The interdimer adsorption opens two dimers and releases two unpaired dimer atoms of high energy, whereas the intradimer addition only saturates one dimer without generating unpaired dimer atoms. This explains the fact that the intradimer features **1** and **2** dominates over the interdimer adducts.

Since Ge(100) has lines of symmetry along the dimer row direction, each phenyl ring has two stable orientations relative to the dimer row direction. Our calculation also proves that the phenyl rings are readily to rotate through single C-N bonds with negligible barriers (<0.3 eV, in Figure S3). This means the conversion between each pair of stable enantiomers can occur at room temperature. Indeed, the dumbbells rotated themselves by 108° and convert to their enantiomers in another scanning round (Figure 1b, inset). Interestingly, there is only one orientation in each scanning run, indicating that the azimuth and tilt angles of phenyl rings can be affected by an external electric field, due to their large polarizability.[41–43] Under a lateral electric field (for example, induced by asymmetrically charged tip covered by molecules in our case), the azimuth angle of phenyl ring can be tuned and led to the uniform orientation, whereas the identical tilt angle of the phenyl rings in Figure 2k and Figure 2i will dissimilate. Such a dissimilation may result in the discrepancies in heights, as well as projected lateral locations between features **3** and **4**. Similar splitting was observed between Features **1** and **2**. Further theoretical work considering the influences of the external electric field and the tip shape will offer new details but out of our scope here. Nevertheless, regardless of the actual binding mechanism (interdimer or intradimer), the phenyl ring planes are always almost perpendicular to the surface and able to present analogous dumbbell-like features under STM.

In the Tersoff-Hammann scheme, constant current images map the local density of states or the accumulation of orbitals of a system at the energy window between E_F and $E_F + eV$, where E_F and V are the Fermi level and tunneling bias, respectively.[7] In our experiments, the bias -1.6 eV is referred to the substrate, thus only the occupied orbitals lower than the substrate Fermi level by <1.6 eV are imaged. To extract which occupied orbitals of the molecule/substrate system contribute to the dumbbell-like features, the partial density of states (PDOS) of the nitrosobenzene fragment in adsorbed state and total DOS (Figure 3) curves are plotted. The real Fermi level of a semiconductor substrate is affected by many factors and does not always coincide with the calculated result. Constant current images at multiple biases or scanning tunneling spectroscopy (STS) spectra may reveal the discrepancy,[22] however was not obtained in our experiments due to limited instrumental functionalities. Nevertheless, in Figures 3a and 3b, the valence band maximum (VBM) of each nitrosoadduct is defined as the nominal Fermi level, lower than the real one, which will always fall in the band gap.

Two nitrosoadducts have similar molecular PDOS curves with many distinct peaks at the same energy, indicating that the molecules in the two different adsorbed states undergo

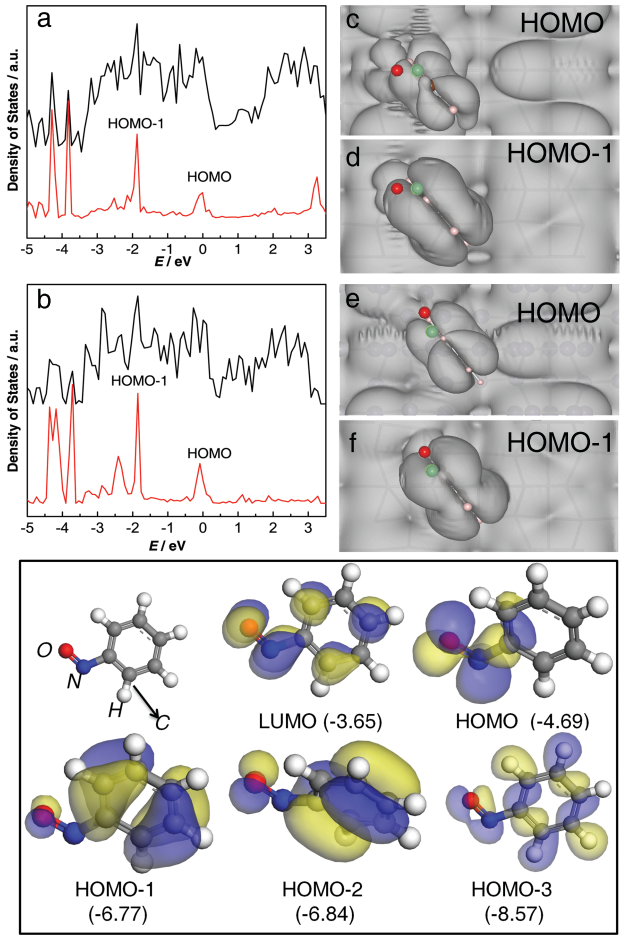

Fig. 3 (a) top: Total DOS of the intradimer nitrosoadduct; bottom: PDOS of nitrosobenzene fragment. (b) top: Total DOS of the interdimer nitrosoadduct; bottom: PDOS of nitrosobenzene fragment. (c) and (d) "HOMO" and "HOMO-1" orbitals in (a). (e) and (f) "HOMO" and "HOMO-1" orbitals in (b). (g) Molecular orbitals of free nitrosobenzene. Isodensity: 0.03 e/Å^3. The energies in parentheses are in the unit of eV relative to the vacuum level. The green and red balls refer to N and O atoms, respectively.

analogous electronic interaction with the substrate. Figures 3a and 3b show that in the nominal bias range, there is only one frontier orbital (marked as "HOMO") of the adsorbed molecule for each adduct. It is this "HOMO" that is responsible for the observed dumbbell-like features. In Figures 3c and 3e, each "HOMO" has a nodal plane (the phenyl ring plane) to separate four lobes to its two sides. However, the orbital lobes at the same side cannot be distinguished in the STM images due to their superimposition along the tunneling direction. The next highest orbitals "HOMO-1" (Figure 3d and 3f) of similar nodal planes may also contribute to the "dumbbells" with less possibility. The deeper orbitals do not contribute to the STM signals as they have much lower energy levels. In short, here our images are highly interesting because they are a "side view" of a single phenyl ring rather than the "top views" of polycyclic aromatics in the previous reports.[13]

Since nitrosobenzene molecules are chemisorbed onto Ge(100) through covalent bonds, the above "HOMOs" and "HOMO-1s" should be the molecule/Ge(100) system orbitals rather than the pure molecular orbitals in free state. This is also the general case for most of organic/semiconductor junctions. However, by comparing these system orbitals with the molecular orbitals of free molecules, it is possible to trace the molecular contribution to these "HOMO" and "HOMO-1" orbitals. Obviously, two "HOMOs" in Figures 3c and 3e resemble the HOMO-1 of free nitrosobenzene (Figure 3g). The nitrosobenzene's HOMO is mainly composed of the N=O double bond, which has been reacted with Ge dimer atoms upon adsorption. Two "HOMO-1" orbitals in Figures 3d and 3f have analogous nodal planes as the HOMO-2 of free nitrosobenzene. In comparison with benzene, nitrosobenzene's HOMO-1 and HOMO-2 orbitals originate from two degenerate π orbitals (mainly composed by six C $2p$ atomic orbitals) of free benzene (Figure S4). Energetically, these two π orbitals split in nitrosobenzene due to the symmetry breakdown by the nitroso group. From the PDOS curves in Figures 3a and 3b, it is found that such spitting remains even though the N=O bond is reacted upon adsorption, indicating the electronic properties of the phenyl fragment are well retained when -N=O is sacrificed as a spacing/attaching group. Figure 3g exhibits that the HOMO-1 and HOMO-2 of nitrosobenzene are mainly distributed on the phenyl ring and it is this part being captured by STM. There is negligible contribution from N and O atoms either before or after adsorption. Therefore we state that the imaged dumbbell-like features correspond to the HOMO-1 (and HOMO-2) orbital of free nitrosobenzene, resembling the π orbitals of benzene.

Conclusion

We successfully resolved the molecular orbitals of nitrobenzene adsorbed on Ge(100) using in situ dosing technique. Nitrosobenzene reacts with Ge(100) via N=O adding to a single dimer or the paired end-bridge of two adjacent surface dimers, resulting in the intradimer and interdimer [2+2] nitrosoadducts. The phenyl rings in both products are spatially separated from the substrate and electronically decoupled from the surface states, thus are resolvable under STM. In this self-decoupling binding mechanism, nitrosobenzene molecules are immobilized on Ge(100) through covalent bonds, therefore allowing facile STM measurements and manipulations. The sufficient thermal stability and mechanical robustness of this kind of organic/semiconductor hybrid system is also more feasible than the physisorption system

for the applications in molecule-based devices. Our work demonstrates that self-decoupling can be achieved by sacrificing a double bond as the spacing group covalently attached to a semiconductor surface. This may be possibly extended to other molecule/substrate systems for orbital-resolving attempts.

Acknowledgement

We thank Prof. Tok E. S. for useful suggestions. We are grateful to the financial support from the Ministry of Education, Singapore (Grant No. R-143-000-462-112) and CREATE-SPURc project, National Research Foundation, Singapore (R143-001-205-592).

Note and References

[a]Department of Chemistry, National University of Singapore, 3 Science Drive 3, Lower Kent Ridge Road, Singapore 117543, Email: chmxugq@nus.edu.sg
[b]Singapore-Peking University Research Centre for a Sustainable Low-Carbon Future, 1 CREATE Way, #15-01, CREATE Tower, Singapore 138602
[c]Department of Physics, National University of Singapore, 2 Science Drive 3, Lower Kent Ridge Road, Singapore 117542
[d]State Key Laboratory for Structural Chemistry of Unstable and Stable Species, College of Chemistry and Molecular Engineering, Peking University, Beijing, P. R. China, 100871

Electronic Supplementary Information (ESI) available: Pixel analysis of tip state transition, calculated rotational barriers of phenyl rings, benzene's molecular orbitals, coordinates of calculation models. See DOI: 10.1039/b000000x/.

References

1 C. Joachim, J. K. Gimzewski and A. Aviram, *Nature*, 2000, **408**, 541–548.
2 G. Ashkenasy, D. Cahen, R. Cohen, A. Shanzer and A. Vilan, *Acc. Chem. Res.*, 2002, **35**, 121–128.
3 J. Repp, G. Meyer, S. M. Stojkovic, A. Gourdon and C. Joachim, *Phys. Rev. Lett.*, 2005, **94**, 026803.
4 W. H. Soe, C. Manzano, A. De Sarkar, N. Chandrasekhar and C. Joachim, *Phys. Rev. Lett.*, 2009, **102**, 176102.
5 J. M. Blanco, F. Flores and R. Pérez, *Prog. Surf. Sci.*, 2006, **81**, 403–443.
6 L. Gross, N. Moll, F. Mohn, A. Curioni, G. Meyer, F. Hanke and M. Persson, *Phys. Rev. Lett.*, 2011, **107**, 086101.
7 J. Tersoff and D. R. Hamann, *Phy. Rev. B*, 1985, **31**, 805–813.
8 P. Liljeroth, J. Repp and G. Meyer, *Science*, 2007, **317**, 1203–1206.
9 P. Liljeroth, I. Swart, S. Paavilainen, J. Repp and G. Meyer, *Nano Lett.*, 2010, **10**, 2475–2479.
10 J. Repp, G. Meyer, S. Paavilainen, F. E. Olsson and M. Persson, *Science*, 2006, **312**, 1196–1199.
11 N. J. Tao, *Nature Nanotech.*, 2006, **1**, 173–181.
12 K. Moth-Poulsen and T. Bjørnholm, *Nature Nanotech.*, 2009, **4**, 551–556.
13 L. Gross, *Nature Chem.*, 2011, **3**, 273–278.
14 J. R. Hahn and W. Ho, *Phys. Rev. Lett.*, 2001, **87**, 196102.
15 C. Weiss, C. Wagner, R. Temirov and F. S. Tautz, *J. Am. Chem. Soc.*, 2010, **132**, 11864–11865.
16 Z. H. Cheng, S. X. Du, W. Guo, L. Gao, Z. T. Deng, N. Jiang, H. M. Guo, H. Tang and H. J. Gao, *Nano Res.*, 2011, **4**, 523–530.
17 G. Kichin, C. Weiss, C. Wagner, F. S. Tautz and R. Temirov, *J. Am. Chem. Soc.*, 2011, **133**, 16847–16851.
18 Z. H. Cheng, S. X. Du, N. Jiang, Y. Y. Zhang, W. Guo, W. A. Hofer and H. J. Gao, *Surf. Sci.*, 2011, **605**, 415–418.
19 Q. M. Guo, M. Huang, Z. H. Qin and G. Y. Cao, *Ultramicroscopy*, 2012, **118**, 17–20.
20 H. T. Zhou, J. H. Mao, G. Li, Y. L. Wang, X. L. Feng, S. X. Du, K. Muellen and H. J. Gao, *Appl. Phys. Lett.*, 2011, **99**, 153101.
21 A. Bellec, F. Ample, D. Riedel, G. Dujardin and C. Joachim, *Nano Lett.*, 2009, **9**, 144–147.
22 F. Mohn, J. Repp, L. Gross, G. Meyer, M. S. Dyer and M. Persson, *Phys. Rev. Lett.*, 2010, **105**, 266102.
23 R. J. Hamers, S. K. Coulter, M. D. Ellison, J. S. Hovis, D. F. Padowitz, M. P. Schwartz, C. M. Greenlief and J. N. Russell, *Acc. Chem. Res.*, 2000, **33**, 617–624.
24 J. H. He, W. Mao, G. Q. Xu and E. S. Tok, *Nat. Commun.*, 2014, **5**, 3721.
25 S. Bent, *Surf. Sci.*, 2002, **500**, 879–903.
26 N. Gergel-Hackett, C. Zangmeister, C. A. Hacker, L. J. Richter and C. A. Richter, *J. Am. Chem. Soc.*, 2008, **130**, 4259–4261.
27 D. Vuillaume, *Proc. IEEE*, 2010, **98**, 2111–2123.
28 F. Tao and S. L. Bernasek, *J. Am. Chem. Soc.*, 2007, **129**, 4815–4823.
29 G. Kresse and J. Furthmuller, *Comput. Mater. Sci.*, 1996, **6**, 15–50.
30 G. Kresse and D. Joubert, *Phy. Rev. B*, 1999, **59**, 1758–1775.
31 J. P. Perdew, K. Burke and M. Ernzerhof, *Phys. Rev. Lett.*, 1996, **77**, 3865–3868.
32 B. Delley, *J. Chem. Phys.*, 1990, **92**, 508.
33 B. Delley, *J. Chem. Phys.*, 2000, **113**, 7756.
34 H. Zandvliet, *Phys. Rep.*, 2003, **388**, 1–40.
35 O. Gurlu, A. van Houselt, W. H. A. Thijssen, J. M. van Ruitenbeek, B. Poelsema and H. J. W. Zandvliet, *Nanotechnology*, 2007, **18**, 365305.
36 R. Zhachuk and S. Pereira, *Phy. Rev. B*, 2009, **79**, 077401.
37 J. A. Nieminen, E. Niemi and K. H. Rieder, *Surf. Sci.*, 2004, **552**, L47–L52.
38 R. Gaspari, S. Blankenburg, C. A. Pignedoli, P. Ruffieux, M. Treier, R. Fasel and D. Passerone, *Phy. Rev. B*, 2011, **84**, 125417.
39 F. Moresco, *Phys. Rep.*, 2004, **399**, 175–225.
40 C. J. Villagomez, T. Zambelli, S. Gauthier, A. Gourdon, C. Barthes, S. Stojkovic and C. Joachim, *Chem. Phys. Lett.*, 2007, **450**, 107–111.
41 J. K. H. Horber, W. Haberle, P. Ruppersberg, M. Niksch, D. P. E. Smith and G. Binnig, *J. Vac. Sci. Technol. B*, 1994, **12**, 2243–2246.
42 W. Guo, S. Du, Y. Zhang, W. Hofer, C. Seidel, L. Chi, H. Fuchs and H.-J. Gao, *Surf. Sci.*, 2009, **603**, 2815–2819.
43 P. A. Lewis, C. E. Inman, F. Maya, J. M. Tour, J. E. Hutchison and P. S. Weiss, *J. Am. Chem. Soc.*, 2005, **127**, 17421–17426.
44 K. A. Perrine, T. R. Leftwich, C. R. Weiland, M. R. Madachik, R. L. Opila and A. V. Teplyakov, *J. Phys. Chem. C*, 2009, **113**, 6643–6653.
45 A. Fink, D. Menzel and W. Widdra, *J. Phys. Chem. B*, 2001, **105**, 3828–3837.
46 P. M. Ryan, L. C. Teague and J. J. Boland, *J. Am. Chem. Soc.*, 2009, **131**, 6768–6774.
47 C. Yang and H. C. Kang, *J. Chem. Phys.*, 1999, **110**, 11029–11037.

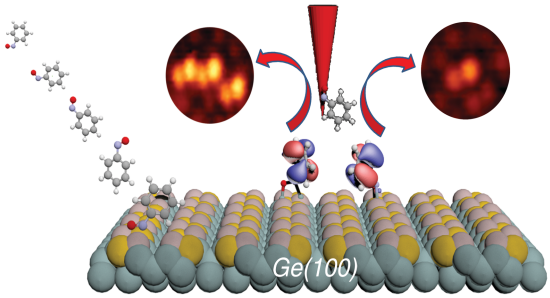

Table of Contents (TOC) Graphic. Molecular orbitals of chemisorbed nitrosobenzene are electronically decoupled from a clean semiconductor substrate and resolved by STM.